The TWIK2 Potassium Efflux Channel in Macrophages Mediates NLRP3 Inflammasome-induced Inflammation

Anke Di[1,*], **Shiqin Xiong**[1,*], **Zhiming Ye**[1], **R.K. Subbarao Malireddi**[2], **Satoshi Kometani**[1], **Ming Zhong**[1], **Manish Mittal**[1], **Zhigang Hong**[1], **Thirumala-Devi Kanneganti**[2], **Jalees Rehman**[1], and **Asrar B. Malik**[1,#]

[1]Department of Pharmacology and the Center for Lung and Vascular Biology, The University of Illinois College of Medicine, Chicago, IL 60612, USA

[2]Department of Immunology, St. Jude Children's Research Hospital, Memphis, TN 38105, USA

SUMMARY

Potassium (K^+) efflux across the plasma membrane is thought to be an essential mechanism for ATP-induced NLRP3 inflammasome activation yet the identity of the efflux channel has remained elusive. Here we identified the two-pore domain K^+ channel (K_{2P}) TWIK2 as the K^+ efflux channel triggering NLRP3 inflammasome activation. Deletion of the *Kcnk6* gene (encoding TWIK2) prevented NLRP3 activation in macrophages and suppressed sepsis-induced lung inflammation. Adoptive transfer of *Kcnk6*$^{-/-}$ macrophages into mouse airways after macrophage depletion also prevented inflammatory lung injury. The K^+ efflux channel TWIK2 in macrophages has a fundamental role in activating the NLRP3 inflammasome and consequently mediates inflammation, pointing to TWIK2 as a potential target for anti-inflammatory therapies.

eTOC Blurb

[#]***Corresponding Author:*** Asrar B. Malik, Department of Pharmacology, The University of Illinois College of Medicine, 835 South Wolcott Avenue, Chicago, IL, 60612, Phone: (312) 996-7635;Fax: (312) 996-1225; abmalik@uic.edu.
[*]These authors contributed equally to this work.
[#]***Lead Contact:*** Asrar B. Malik, Department of Pharmacology, The University of Illinois College of Medicine, 835 South Wolcott Avenue, Chicago, IL, 60612, Phone: (312) 996-7635;Fax: (312) 996-1225; abmalik@uic.edu

SUPPLEMENTAL ITEM TITLES
Supplemental Figure S1,S2, S3,S4,S5 and S6
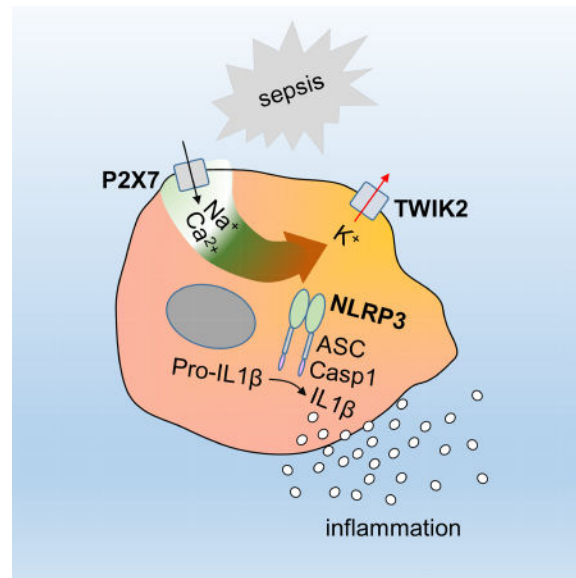
Potassium efflux is required for NLRP3 inflammasome activation, however the channel mediating the efflux has remained elusive. Malik et al. identify the potassium channel TWIK2 as a mediator of potassium efflux and NLRP3 activation in macrophages. Targeting TWIK2 could form the basis for therapeutic approaches in inflammatory injury.

INTRODUCTION

Inflammasomes are key components of the host-defense system and essential inflammatory signaling platforms responsible for detecting injury mediators released during infections and tissue damage to activate the inflammatory response (Latz et al., 2013). The inflammasome NLRP3 (Nucleotide-binding oligomerization domain-Like Receptor containing Pyrin domain 3) in macrophages plays a key role in the adaptive inflammatory response as well as pathogenesis of diseases characterized by an excessive maladaptive inflammatory activation such as acute lung injury (dos Santos et al., 2012; Grailer et al., 2014; Wu et al., 2013). NLRP3 inflammasome assembly forms a multimeric protein complex that activates caspase-1, and thereby proteolytically cleaves substrates such as the pro-interleukin-1β (IL-1β) into active pro-inflammatory mediators in response to pathogens and endogenous danger signals (Schroder and Tschopp, 2010). NLRP3 activation is comprised of an initial priming phase involving NF-κB-dependent transcription of NLRP3 and pro-interleukin-1β initiated by pro-inflammatory cytokines or via stimulation of Toll-like receptor (TLR) by agonists such as lipopolysaccharide (LPS) (Burns et al., 2003). The second phase of NLRP3 activation is initiated by Pathogen-Associated Molecular Patterns (PAMPs) or Danger-Associated Molecular Patterns (DAMPs) such as ATP, which ligates the purinergic receptor P2x7 (Surprenant et al., 1996). Although reactive oxygen species (ROS), mitochondrial and lysosomal damage, formation of large cell membrane pores, and increased cytosolic Ca^{2+} can contribute to NLRP3 activation (Latz et al., 2013), studies have shown that the decrease in intracellular K^+ is an essential trigger for NLRP3 activation induced by ATP and other DAMPs (Franchi et al., 2007; Petrilli et al., 2007) and this has been subsequently confirmed

by later studies (Munoz-Planillo et al., 2013). However, the identity of the K^+ efflux channel which enables the requisite decrease in intracellular K^+, the mechanisms of its activation, and its significance in the pathogenesis of inflammation have remained enigmatic.

The purinergic P2x7 receptor (Chessell et al., 1998; Rassendren et al., 1997; Surprenant et al., 1996) is a non-selective cation channel with a pore-forming motif resembling K^+ channels (Valera et al., 1994), and has thus been proposed as a putative K^+ efflux channel mediating activation of NLRP3 inflammasome (Chen and Nunez, 2010; Pelegrin and Surprenant, 2009). However, this would require that P2x7 receptor function both as a DAMP sensor and a K^+ efflux channel. Here, we demonstrate that K^+ efflux regulates ATP-induced NLRP3 activation in macrophages through the K^+ channel TWIK2 (Two-pore domain Weak Inwardly rectifying $\underline{K}^+$ channel 2) (Enyedi and Czirjak, 2010). Genetic deletion of the *Kcnk6* gene (encoding TWIK2) and pharmacologic inhibition of TWIK2 with quinine abrogated NLRP3 activation and inflammatory lung injury in mice challenged with endotoxin or polymicrobial sepsis. Furthermore, adoptive transfer of *Kcnk6*$^{-/-}$ macrophages into wild type mice depleted of lung macrophages prevented sepsis-induced NLRP3 inflammasome activation and inflammatory lung injury. Thus, K^+ efflux through TWIK2 in macrophages is an essential mechanism of ATP-induced NLRP3 inflammasome activation and sepsis-induced lung injury.

RESULTS

TWIK2 deficiency inhibits NLRP3 inflammasome activation in macrophages

Since a decrease in cytosolic K^+ is an important trigger for NLRP3 activation (Franchi et al., 2007; Petrilli et al., 2007), we sought to identify the K^+ efflux channel responsible for ATP-induced NLRP3 activation using various pharmacologic K^+ channel inhibitors. We activated the NLRP3 inflammasome with extracellular ATP in mouse bone marrow derived macrophages (BMDMs) primed with LPS (Burns et al., 2003). NLRP3 inflammasome activation was evaluated by measuring caspase 1 activation (p20 subunit of caspase 1) by immunoblotting and IL-1β release by ELISA. Concentrations of ATP were chosen based on establishing dose- and time-dependent responses of ATP-induced IL-1β release and caspase 1 activation in BMDMs (Figures S1A – C). We first studied known pharmacologic K^+ channel inhibitors, Ba^{2+} (inhibitor of inward rectifier K^+ channels), tetraethylammonium (TEA, inhibitor of voltage gated K^+ channels), Iberiotoxin (IbTX, inhibitor of large-conductance calcium-activated K^+ channels, BK) and quinine (inhibitor of two-pore domain K^+ channels, K_{2P}) (Shieh et al., 2000) (Figure S2A). We found that only quinine prevented caspase 1 activation in BMDMs in a concentration-dependent manner (Figures 1A – B) and that it also suppressed the ATP-induced IL-1β release (Figure 1C and Figure S2A). In addition, quinine inhibited the outward current in BMDMs induced by ATP (Figure S2B), whereas chloroquine, a related quinoline compound (Leed et al., 2002), had no inhibitory effect on the ATP-induced current (Figure S2B), and minimally affected IL-1β maturation and caspase 1 activation (Figure S3). Quinine also suppressed ATP-induced cytotoxicity as evaluated by the release of tumor necrosis factor alpha (TNFα) and release of lactate dehydrogenase (LDH) (Chan et al., 2013) (Figure S4).

We next focused on K^+ channels of the K_{2P} family since it is known that members of this family are quinine sensitive (Shieh et al., 2000). The K_{2P} family is divided into six subfamilies (TWIK, TREK, TASK, TALK, THIK, and TRESK) with each having different members (Enyedi and Czirjak, 2010). Quantitative expression analysis of K_{2P} channels in BMDMs demonstrated that mRNA levels of *Kcnk6* (encoding TWIK2), *Kcnk2* (encoding TREK1), and *Kcnk12* (encoding THIK2) were the highest as compared to the others (Figure 1D). We then depleted each of these channels by siRNA in J774A.1 mouse macrophages and assessed effects of gene depletion on inflammatory activation. Only *Kcnk6* depletion reduced IL-1β maturation and release (Figures 1E and 1F). *Kcnk6* depletion also decreased caspase 1 activation (Figure 1F) in response to ATP, indicating the importance of TWIK2 (encoded by *Kcnk6*) for NLRP3 inflammasome activation. Furthermore, inhibition of NLRP3 activation by *Kcnk6* depletion in siRNA treated BMDMs also reduced oligomerization of apoptosis-associated speck-forming protein containing caspase-recruiting domain (ASC), the adaptor protein bridging NLRP3 and caspase 1 to form inflammasome complexes (Lu et al., 2014; Srinivasula et al., 2002) (Figure 1F).

TWIK2 activates P2x7 independent K⁺ efflux in macrophages

We next determined the electrophysiological mechanism by which TWIK2 deficiency suppressed NLRP3 activation and assessed the ATP-induced whole cell current using a patch clamp approach. Since the P2x7 receptor is an ATP-gated non-selective cation channel with a pore-forming motif resembling K^+ channels (Valera et al., 1994), we examined whether the P2x7 receptor could itself mediate K^+ efflux and therefore contribute to ATP-induced NLRP3 inflammasome activation. Voltage clamping was performed in BMDMs obtained from wild type (*Wt*), P2x7 receptor-deleted (*P2rx7⁻/⁻*) and TWIK2 deleted (*Kcnk6⁻/⁻*) mice, with K^+ as the major outward current carrier and Na^+ and Ca^{2+} as the major inward current carriers. Representative time courses of current and voltage (*I-V*) plot with a ramp protocol are shown in Figures 2A – F and *I–V* plots of the peak currents are shown in Figures 2G and 2H shows results of adding quinine in the recording solution (bath solution). The amplitude of both peak inward currents and outward currents are summarized in Figure 2I. ATP (5 mM) rapidly induced whole cell currents (patch clamp recordings of unstimulated cells are shown in Figure S5A–C), with both inward and outward currents reaching their peaks within 20s in wild-type (WT) BMDMs (Figure 2A) and then declining to the basal state in ~60s (Figures 2A and 2B). Quinine inhibited only the outward currents induced by ATP (Figure 2H). As expected, the inward current was inhibited in macrophages from *P2rx7⁻/⁻* mice when compared to those from WT mice (Figures 2C, 2D, and 2G). The outward currents observed in WT BMDMs persisted in *P2rx7⁻/⁻* BMDMΦ, but with a slower developing rate (reaching its peak in 80s, Figure 2C). This outward K^+ current was quinine-sensitive (Figure 2H). In *Kcnk6⁻/⁻* BMDMs, however, the ATP-induced inward currents were intact but had a slower developing rate (in ~90s) as compared to BMDMs from WT mice (Figures 2 E, F, G) and the current was insensitive to quinine (Figure 2H). The outward currents in *Kcnk6⁻/⁻* BMDMs were reduced (Figures 2E, F and G) when compared to both, *WT* and *P2rx7⁻/⁻* BMDMs. These results demonstrate the requisite role of TWIK2 in mediating the ATP-induced K^+ efflux current in BMDMs.

TWIK2 mediated K⁺ efflux is required for ATP-induced NLRP3 inflammasome activation

We next investigated whether TWIK2 also regulates NLRP3 inflammasome activation by other PAMPs such as imiquimod which activates NLRP3 inflammasome independent of K^+ efflux (Gross et al., 2016), and nigericin, a bacterial pore-forming toxin (a K^+ ionophore), which induces NLRP3 activation via enhancing K^+ efflux independent of P2x7 (Katsnelson et al., 2015). We demonstrated the requisite role for TWIK2 in ATP-induced NLRP3 inflammasome activation as caspase 1 activation and IL-1β and IL-18 release were inhibited in TWIK2-deficient BMDMs (obtained from *Kcnk6⁻/⁻* mice) whereas neither nigericin (which induced a small outward current, Figure S5 D–E) nor imiquimod-induced NLRP3 inflammasome activation was affected in WT BMDMΦ when compared to the activation seen *Kcnk6⁻/⁻* BMDMs (Figures 3A–C). *Kcnk6⁻/⁻* BMDMs also demonstrated reduced ATP induced cytotoxicity as evaluated by release of LDH and TNFα, whereas nigericin and imiquimod-induced cytotoxicity were unaffected by TWIK2 deletion (Figure S6 A–B). We next determined whether *Kcnk6⁻/⁻* BMDMs responded to triggers for other inflammasomes such as AIM2 (Absent In Melanoma 2), NLRC4 (Nucleotide-binding oligomerization domain-Like Receptor family caspase-recruiting domain containing 4), and pyrin inflammasomes (Broz and Dixit, 2016). We found that the responses of *Kcnk6⁻/⁻* BMDMs to *Salmonella, Poly (dAdT)* and *TcdB toxin*, which respectively activate NLRC4, AIM2 and pyrin inflammasomes, remained intact (Figures 3D –3E). Release of TNFα in response to these non-NLRP3 inflammasome triggers was also preserved in *Kcnk6⁻/⁻* BMDMs (Figure 3F).

We also addressed the K^+ efflux mechanism in TWIK2-mediated NLRP3 inflammasome activation by determining the intracellular K^+ concentration in cells challenged with ATP. ATP-challenge induced a marked drop in intracellular K^+ concentration in WT mice consistent with ATP-induced K^+ efflux but this decrease was absent in *Kcnk6⁻/⁻* BMDMs (Figure 3G). These results thus demonstrate a specific role for TWIK2 in mediating ATP-induced NLRP3 inflammasome activation by enabling K^+ efflux.

Macrophage TWIK2 is required for sepsis-induced NLRP3 inflammasome activation and inflammation

To next address the role of TWIK2-mediated inflammasome activation in inducing inflammation, we used two complementary models of lung inflammation and injury in mice, Cecal Ligation Puncture (CLP) which causes polymicrobial sepsis (Cuenca et al., 2010) as well as endotoxemia induced by systemic injection of bacterial lipopolysaccharide (LPS) (Bachmaier et al., 2007). Lungs from *Kcnk6⁻/⁻* mice challenged with CLP showed inhibition of NLRP3 inflammasome activation as evaluated by caspase 1 activation and IL-1β maturation (Figure 4A – 4C). We also observed a marked decrease in endotoxemic inflammatory lung injury in *Kcnk6⁻/⁻* mice as evaluated by the histopathology of lungs, quantification of neutrophil and macrophage infiltration in the alveoli (Figures 4D and 4E) and myeloperoxidase (MPO) activity of lung tissue (Figure 4F).

To identify the *in vivo* role of macrophage TWIK2 in the regulation of NLRP3 inflammasome activation and inflammation, we first depleted endogenous mouse lung macrophages with liposomal clodronate (Weisser et al., 2012) (see Figure S6C), and

subsequently performed an adoptive transfer (i.t.) of BMDMs from either wild type TWIK2 (*Kcnk6$^{+/+}$*) or *Kcnk6$^{-/-}$* mice (Figure 4G). We then induced endotoxemia in recipient mice. The mice receiving *Kcnk6$^{-/-}$* macrophages showed significantly reduced NLRP3 inflammasome activation (Figures 4H – 4J) and MPO activity (Figure 4K) as compared to mice receiving *Kcnk6$^{+/+}$* macrophages.

Cooperation of P2x7 receptor and TWIK2 in NLRP3 inflammasome activation

Since P2x7 receptor deficiency has been shown to abolish IL-1β maturation (de Torre-Minguela et al., 2016; Munoz-Planillo et al., 2013; Solle et al., 2001), we next addressed the possibility that P2x7 receptor and TWIK2 can independently regulate NLRP3 inflammasome activation and inflammation. Thus, we performed experiments using *Kcnk6$^{-/-}$*, *P2rx7$^{-/-}$*, and *Nlrp3$^{-/-}$* mice and determined NLRP3 inflammasome activation. We observed a marked decrease in endotoxemic inflammatory lung injury in both *Kcnk6$^{-/-}$* mice and *P2rx7$^{-/-}$* mice, comparable to what was observed in *Nlrp3$^{-/-}$* mice as assessed by neutrophil and macrophage infiltration in the alveoli (Figures 5A and 5B) as well as by quantification of myeloperoxidase (MPO) activity in the lungs (Figure 5C). The inflammatory cytokines IL-1β, IL-18, and TNFα in serum were also significantly reduced in *Kcnk6$^{-/-}$*, *P2rx7$^{-/-}$*, and *Nlrp3$^{-/-}$* mice (Figures 5D – 5F). Caspase 1 activation, an indicator of NLRP3 activation, and the generation of mature IL-1β were completely inhibited in *Kcnk6$^{-/-}$*, *P2rx7$^{-/-}$*, and *Nlrp3$^{-/-}$* mice upon LPS challenge (Figure 6A). We also observed that ATP - induce IL-1β release was significantly decreased in macrophages from either *P2rx7$^{-/-}$* or *Kcnk6$^{-/-}$* mice (Figure 6B). These results thus demonstrated that the phenotype observed with TWIK2 deletion was similar to that seen with P2x7 receptor deletion in mediating NLRP3 inflammasome activation and inflammation.

Thus, we hypothesized that P2x7 receptor-mediated influx of cations facilitates K$^+$ efflux through TWIK2 by changing the membrane potential, since the membrane potential drives K$^+$ efflux (David J. Aidley, 1996). We validated this hypothesis by varying ion concentrations and measuring IL-1β release in macrophages. We observed that higher extracellular concentrations of K$^+$ prevented IL-1β release (Figure 6C). However, IL-1β release was only partially blocked in cells bathed in a nominally Ca^{2+} free or nominally Na$^+$ free solution and was fully inhibited in cells bathed in a solution in which both Ca^{2+} and Na$^+$ are nominally free (Figure 6C). These findings suggest a cooperative role for both P2x7 and TWIK2 in which the former enables Ca^{2+} and Na$^+$ influx to change the membrane potential and the latter enables K$^+$ efflux to activate NLRP3 inflammasome.

DISCUSSION

The activation of NLRP3 inflammasome in response to microbial infection contributes to host defense by activating an immune response and thereby serves to limit microbial invasion. However, excessive or dysregulated activation of the inflammasome pathway can also result in tissue injury and autoimmune disorders (Franchi et al., 2012). Activation of NLRP3 induces caspase 1-mediated secretion of the pro-inflammatory cytokine IL-1β and pyroptosis (Latz et al., 2013), and has a critical role in mediating tissue damage such as acute lung injury during systemic infections (Howrylak and Nakahira, 2017). Extracellular

ATP acts as a danger signal because it indicates the release of intracellular ATP into tissue as a consequence of cell death. ATP triggers the efflux of K^+ from macrophages resulting in NLRP3-mediated activation of caspase 1 and production of IL-1β, which in turn can activate adaptive and maladaptive inflammatory responses (Howrylak and Nakahira, 2017). Although it has been proposed that that P2x7 receptor itself may serve as a channel mediating K^+ efflux in ATP-induced inflammasome activation (Chen and Nunez, 2010; Franchi et al., 2007; Kahlenberg and Dubyak, 2004; Pelegrin and Surprenant, 2006, 2009), this notion has mostly been based on the role of P2x7 as an ATP receptor and external application of ATP rendering the cell membrane permeable to several cations K^+, Ca^{2+}, Na^+ (Buell et al., 1996; Chessell et al., 1998; Hume and Thomas, 1988; Rassendren et al., 1997) and even to anions (Thomas and Hume, 1990). However, few studies have directly assessed the role of P2x7 receptor in regulating ATP-induced K^+ efflux across the plasma membrane. Here, using patch clamp analysis to monitor ATP-induced current as well as directly measuring intracellular K^+ concentration in cells from both wild type and $Kcnk6^{-/-}$ mice as well as $P2rx7^{-/}$ mice, we identified TWIK2 as an ATP-responsive K^+ efflux channel. Using a screen for candidate K^+ channels, gene expression analysis and targeted gene depletion of TWIK2 in mice, we established the requisite role of TWIK2 in regulating ATP-induced NLRP3 inflammasome activation and sepsis-induced inflammatory lung injury. Further we observed that depletion of lung macrophages with clodronate (Weisser et al., 2012) in mice and subsequent adoptive transfer of $Kcnk6^{-/-}$ macrophages into lungs significantly reduced NLRP3 activation and inflammatory lung injury induced by sepsis. These results support an exclusive role of TWIK2 in macrophages as the efflux K^+ channel mediating NLRP3 inflammasome activation and sepsis-induced inflammation.

Our data suggest that TWIK2 and P2x7 receptor function in cooperation to regulate NLRP3 inflammasome activation. Cooperation between P2x7-mediated influx of Ca^{2+} and Na^+ and TWIK2-mediated K^+ efflux was demonstrated by observing the slow activation of the outward current in the absence of the P2x7 receptor and slow activation of the inward current in the absence of TWIK2 channel (Figures 2A – 2F). The P2x7 receptor senses tissue injury as an ATP receptor and acts as a non-selective ion channel which enables influx of cations. Cation influx in turn modifies the membrane potential to generate the driving force favoring efflux of K^+. This model of regulation provides important insights into how innate immune signaling receptors such as Pattern Recognition Receptors (PRRs) monitor signs of infection, damage, and other forms of cellular stress to trigger inflammasome formation and activation and mount cellular immune responses (Latz et al., 2013). As a PRR, P2x7 receptor serves as a sensor for DAMPs such as ATP but, as shown by our studies, it requires TWIK2 as an executioner to initiate NLRP3 inflammasome activation. This cooperative function between the two provides the cell with an additional layer of control to regulate both injury sensing and executioner responses.

TWIK2 (encoded by $Kcnk6$) is a member of the two-pore domain K^+ channel (K_{2P}) family (K_{2P} 6.1) that gives rise to background K^+ currents responsible for stabilizing the negative resting membrane potential and counterbalancing depolarization (Enyedi and Czirjak, 2010). TWIK2 is highly expressed in cells of the immune, vascular, and gastrointestinal systems (Patel et al., 2000). Although human and rat TWIK2 have been cloned and electrophysiological properties have been studied in heterologous expression systems

(Chavez et al., 1999; Lloyd et al., 2009; Patel et al., 2000), the physiological functions of TWIK2 are poorly understood (Lloyd et al., 2011). Human TWIK2 expressed heterologously in *Xenopus* oocytes is constitutively active and insensitive to quinine (Chavez et al., 1999) whereas rat TWIK2 heterologously expressed in COS cells is inhibited by quinine (Patel et al., 2000) and the channel activity is enhanced by arachidonic acid (Lloyd et al., 2009). We did not observe a TWIK2 mediated constitutively active background K^+ current in mouse BMDMs (or it was too small to be recorded) whereas we observed that ATP-induced currents were in part mediated by TWIK2, indicating ATP is involved in the gating of TWIK2 channel. How ATP regulates TWIK2 activity is not clear. Recently, a TWIK2 study in the vasculature (Lloyd et al., 2011) suggested that TWIK2 deficiency induces vascular dysfunction and hypertension through a mechanism involving smooth muscle cell depolarization and enhanced Rho kinase activity (Lloyd et al., 2011; Pandit et al., 2014). These results suggest that TWIK2 has a beneficial signaling role in vascular smooth muscle cells. Our study demonstrates that the endogenous expressed mouse TWIK2 in macrophages is activated by ATP and sensitive to quinine. In our model, TWIK2 regulates cell immunity by expression in the plasma membrane as a K^+ efflux channel responsible for the ATP-induced NLRP3 inflammasome activation and therefore participates in the regulation of inflammation induced by PAMPs. Another recent study has shown that TWIK2 generates background K^+ currents in endolysosomes and thus regulates the number and size of lysosomes (Bobak et al., 2017). TWIK2 contains sequence signals responsible for the expression of TWIK2 in the Lamp1-positive lysosomal compartment (Bobak et al., 2017), and sequential inactivation of these trafficking motifs abolishes the targeting of TWIK2 to lysosomes, thus promoting functional relocation of the channel to the plasma membrane (Bobak et al., 2017). Since the K^+ concentration in lysosome is lower than in the cytosol (Wang et al., 2017), lysosomal TWIK2 activation could be an alternative pathway of NLRP3 inflammasome activation, which may decrease cytosolic K^+ concentrations through transferring K^+ from the cytosol into lysosomal lumen following its concentration gradient upon activation. This notion raises the intriguing question whether redistribution of K^+ in intracellular compartments may also activate the NLRP3 inflammasome similar to what is seen with K^+ efflux to the extracellular space.

The present study identifies TWIK2 as a key regulator of the inflammatory response in macrophages. It is also of interest that TWIK2-induced responses in macrophages were inhibited by quinine which has been used as an antiarrhythmic drug (Sheldon et al., 1995) but gained widespread historical usage in the 18th–19th centuries as the anti-malaria drug that was also used for other tropical fevers (Achan et al., 2011). Our findings might provide some insights into its efficacy because we observed that inhibition of TWIK2 suppressed NLRP3 inflammasome activation and release of the fever-inducing cytokine IL1β. This is not only of mere historical interest but points to a major translational application of TWIK2. Targeted TWIK2 inhibitors with minimal antiarrhythmic side effects could be developed as therapeutics for severe inflammatory injury or autoimmune diseases involving NLRP3 activation. In summary, our results define TWIK2 as an essential K^+ efflux channel in macrophages and provide mechanistic insights into ATP-induced NLRP3 inflammasome activation and lung inflammation.

STAR METHODS

CONTACT FOR REAGENT AND RESOURCE SHARING

Further information and requests for resources and reagents should be directed to and will be fulfilled by the Lead Contact, Asrar B. Malik (abmalik@uic.edu)

EXPERIMENTAL MODEL AND SUBJECT DETAILS

Cells—Mouse bone marrow derived macrophage (BMDMs) and mouse J774A.1 macrophage cell line (ATCC (TIB-67™) were used.

Mice—C57 black 6 (C57BL/6) mice were obtained from Charles River Laboratory. *Kcnk6$^{-/-}$* mice was a generous gift from Dr. Lavannya M. Pandit (Baylor College of Medicine) (Lloyd et al., 2011; Pandit et al., 2014). *P2rx7$^{-/-}$, Nlrp3$^{-/-}$* and *Caspase 1$^{-/-}$* mice were purchased from Jackson Laboratory. All mice were housed in the University of Illinois Animal Care Facility in accordance with institutional and NIH guidelines. Veterinary care and animal experiments were approved by the University of Illinois Animal Care & Use Committee.

METHOD DETAILS

Cell cultures—Mouse bone marrow derived macrophage (BMDMs) were induced and cultured as described (Zhang et al., 2008). The mouse J774A.1 macrophage cell line was obtained from ATCC (TIB-67™) and was cultured and propagated as described (Di et al., 2001).

Mouse endotoxemia and polymicrobial sepsis model—For LPS-induced endotoxemia, mice received a single intraperitoneal dose (20 mg/kg) of LPS (Escherichia coli 0111:B4, L2630, Sigma). Polymicrobial sepsis was induced by cecal ligation puncture (CLP) as previously described (Cuenca et al., 2010) with 2 punctures and 0.5 cm ligation length using a 16-gauge needle.

Whole cell recordings—Electrophysiological recordings were obtained using a voltage-clamp technique. All experiments were conducted at room temperature ($22 - 24^0$ C) using an EPC-10 patch clamp amplifier (HEKA Electronik GmbH, Lambrecht, Germany) and using the Pulse V 8.8 acquisition program (HEKA Electronik GmbH, Lambrecht, Germany). Whole cell currents were elicited by using a ramp protocol with test pulse range from -100 to $+ 50$ mV (200 ms in duration). The holding potential was 0 mV. The pipette solution contained (in mM): 120 K-glutamic acid, 2 Ca-Acetate Hydrate, 2 Mg-SO4, 33 KOH, 11 EGTA and 10 Hepes, pH 7.2. The bath solution contained (in mM): 140 Na-glutamic acid, 2 Ca-Acetate Hydrate, 1 Mg-SO4, 10 HEPES, pH 7.4. Whole cell currents were analyzed using IGOR software (WaveMetrics, Lake Oswego, OR).

Solutions used in ion-replacement experiments—Nominally K$^+$ free solution contains (in mM): 150 NaCl, 2 CaCl$_2$, 1 MgCl$_2$, 10 Hepes; 5 mM K$^+$ solution contains (in mM): 5 KCl, 145 NaCl, 2 CaCl$_2$, 1 MgCl$_2$, 10 Hepes; 50 mM K$^+$ solution contains (in mM): 50 KCl, 100 NaCl, 2 CaCl$_2$, 1 MgCl$_2$, 10 Hepes; 150 mM K$^+$ solution contains (in mM):

150 KCl, 2 CaCl$_2$, 1 MgCl$_2$, 10 Hepes; Nominally K$^+$, Na$^+$ free solution contains (in mM): 150 NMDG - HCl, 2 CaCl$_2$, 1 MgCl$_2$, 10 Hepes; Nominally K$^+$, Ca^{2+} free solution contains (in mM): 150NaCl, 1 MgCl$_2$, 10 Hepes; Nominally K$^+$, Na$^+$, Ca^{2+} free solution contains (in mM): 150 NMDG - HCl, 1 MgCl$_2$, 10 Hepes.

Quantitative RT-PCR for K$^+$ channel expression in BMDMs—Total RNA of cultured BMDMs was extracted using the RNeasy Micro Kit (Qiagen) according to the manufacturer's instructions. RNA isolated from BMDMs was converted to cDNA using the High-Capacity cDNA Reverse Transcription Kit (Applied Biosystems). Real-time PCR was performed using SYBR Green Master Mix on ViiAZ (Applied Biosystems) according to the manufacturer's protocols. The following primers were used for PCR: TASK1 (KCNK3): forward, 5'-CGGCTTCCGCAACGTCTAT-3', and reverse, 5'-TTGTACCAGAGGCACGAGCA-3'; TASK2 (KCNK5): forward, 5'-CCGGGGTCCTTTACTCACCT-3', and reverse, 5'-GTTCCAGTTGTTGAAAGTCTGGT-3'; TASK3 (KCNK9): forward, 5'-GACGTGCTGAGGAACACCTACTT-3', and reverse, 5'-GTGTGCATTCCAGGAGGGA-3';TALK1 (KCNK16): forward, 5'-CTTCTGGCCTATATCTGCTACC-3', and reverse, 5'-GGAACTGGTCCCTGGATTGAG-3'; TWIK1(KCNK1): forward, 5'-AGCAACGCCTCGGGAAAT-3', and reverse, 5'-GAGGAGGGTGAACGGGAT-3'; TWIK2 (KCNK6): forward, 5'-CTGGTCCTATGGTGATGC-3', and reverse, 5'-GTCCCAAAGGTAGAGTGA-3'; TWIK3 (KCNK7): forward, 5'-TTGGGGCTGTGGTGCTTC-3', and reverse, 5'-GGCAGATCCCAGTTGCTTGT-3'; TREK1 (KCNK2): forward, 5'-CCACCATCATCTTCATCCTG-3', and reverse, 5'-CCAGCCTTCTATGTGCTTGA-3'; TREK2 (KCNK10): forward, 5'-GAAAGCAGGTGAACTGGGAT-3', and reverse, 5'-GAGTCGAGGAACAGGGTGAT-3'; THIK2 (KCNK12): forward, 5'-GGGACTTCCCTGGAGCCTTC-3', and reverse, 5'-GTCATGCCGAAACCTATGGTCG-3'; TRAAK (KCNK4): forward, 5'-ATGGAGAGCTGGAGCAAGTT-3', and reverse, 5'-GCTGGTAGGCTGGAGAGTTC-3'; IRK1(KCNJ2): forward, 5'-ATGGGCAGTGTGAGAACCAAC-3', and reverse, 5'-TGGACTTTACTCTTGCCATTCC-3'; BK (KCNMA1): forward, 5'-TCTCAGCATTGGTGCCCTCGTAAT-3', and reverse, 5'-GTAGAGGAGGAAGAACACGTTGAA-3'; GAPDH: forward, 5'-CATGGCCTTCCGTGTTC-3', and reverse, 5'-CTGCTTCACCACCTTCTT-3'. The data were analyzed using the comparative cycle-threshold (CT) method, where the amount of target is normalized to an endogenous reference gene, GAPDH.

Silencing of Kcnk6, Kcnk12 and Kcnk2—The siRNAs targeting mouse TWIK2 (*Kcnk6* - L-058227-00-0005), THIK2 (*Kcnk12* - L-062855-00-0005), TREK1 (*Kcnk2* - L-047199-00-0005) and a siRNA negative control (Non-targeting pool siRNA, D-001810-10-20) were obtained from Dharmacon. Transient transfections of these siRNAs into mouse MΦs (J774A.1 cell line) were performed with Amaxa mouse macrophage nucleofector kit (VPA-1009, Lonza) and DharmaFECT 4 Transfection Reagent (T-2004-01, Dharmacon) according to the manufacturer's protocol. To evaluate the efficiency of channel silencing, channel expression was examined with Western blot and inflammasome activation

was examined by measuring p20 intensity via Western blot and IL-1β release through ELISA as mentioned above in cells 2–3 days after transfection.

Evaluation of NLRP3 inflammasome activation in BMDMs and lungs—Prior to experimental treatments, BMDMs incubated with 1 μg/ml LPS as priming signal to induce NF-κB–dependent upregulation of pro–IL-1β and NLRP3 expression (Katsnelson et al., 2015). The cells were primed with LPS for 3 h at 37°C and then priming medium was replaced with either normal culture medium or different bath solutions with different combinations of cations and anions as used and described in 'whole cell recordings" section. To evaluate the NLRP3 inflammasome activation, BMDMs were stimulated with either 5 mM ATP, 10μg/ml Imiquimod or 10μg/ml Nigericin for 30 min at 37°C and then IL-1 β (and/or IL-18) release in the medium or bath solutions were measured by ELISA and Caspase 1 activation was evaluated by Western blot using p20 antibody of Caspase 1. Briefly, cell-free supernatants were collected and then assayed for murine IL-1β (MLB00C, R&D Systems) and IL-18 (7625, MBL) by ELISA kit (R&D Systems) according to the manufacturer's protocol and the adherent BMDMs were collected to generate whole-cell lysate. Cell lysate samples and lung protein samples from mice were subjected to SDS-PAGE and transferred to membrane for Western blot analysis using various primary antibodies (Caspase 1 (p20), IL-1β and TWIK2).

Evaluation of cytotoxicity by LDH release—Bone marrow-derived macrophages (BMDMs) were treated with either quinine (100 μm) or choloroquine (100 μm) for 30 min prior to LPS (1 μg/ml) priming for 3h. Cells were then stimulated with ATP (5 mM) for 30 min. The supernatants of the untreated and treated cells were collected for analysis of LDH activity. 50 μl of supernatant samples were transferred to a 96-well plate. 50 μl of the CytoTox 96® reagent was added to each well and incubated for 30 min. The absorbance signal was measured at 490 nm in a plate reader. Cytotoxicity was calculated according to the manufacturer's instructions.

Measurement of intracellular potassium concentration—The intracellular K^+ concentrations of BMDMs isolated from $Kcnk6^{+/+}$ or $Kcnk6^{-/-}$ mice were measured by the FluxOR™ II green potassium ion channel assay (Invitrogen) as previously described (Wegiel et al., 2014). Briefly, cells were primed with LPS (1 μg/ml) for 3h, and treated with ATP (5 mM) for 30 min. A potassium channel stimulus buffer was added for the fluorescence measurements at 480 nm of excitation wavelength and 530 nm of emission wavelength.

ELISA analysis—IL-1β and TNF-α in mice serum and cell-free supernatants were measured by Quantikine® sandwich ELISA kits (R&D Systems) according to the manufacturer's instructions. IL-18 was measured by MBL ELISA kit. The cytokine concentration of the properly diluted or undiluted samples in 96-well plates was measured at 450 nm wavelength of absorbance, and calculated by GraphPad Prism linear regression analysis.

Assay of ASC oligomerization—Lung tissue or BMDMs lysates were separated into detergent-soluble and detergent-insoluble fractions by centrifugation at 13,000 rpm for 10

min at 4°C. The detergent-insoluble lysate pellet was washed twice with 600 μl ice-cold PBS containing proteinase inhibitor and then suspended in 800 μl PBS containing 2 mM DSS (from a stock 20 mM DSS solution in DMSO). The resuspended detergent-insoluble fractions were incubated with DSS for 30 min at room temperature, repelleted by centrifugation at 9000 rpm for 15 min at room temperature, and the DSS supernatant solution was removed. The DSS-treated pellets were suspended in lysis buffer with proteinase inhibitor. Protein concentration was determined by BCA method. Protein samples were added in SDS-PAGE sample buffer and extracted at 90°C for 10 min. The DSS-treated fractions were resolved by SDS-PAGE, transferred to polyvinylidene fluoride membrane, and analyzed by anti-ASC antibody by Western blotting.

Myeloperoxidase (MPO assay)—The lungs were homogenized in 1 mL of PBS with 0.5% hexadecyltrimethylammonium bromide. The homogenates were sonicated, centrifuged at $40,000 \times g$ for 20 min, and run through two freeze-thaw cycles. The samples were homogenized and centrifuged a second time. The supernatant was then collected and mixed 1/30 (vol/vol) with assay buffer (0.2 mg/mL o-dianisidine hydrochloride and 0.0005% H_2O_2). The change in absorbance was measured at 460 nm for 3 min, and MPO activity was calculated as the change in absorbance over time.

Alveolar macrophage depletion and reconstitution—Commercially available clodronate liposomes (Clodrosome) were administered directly into lungs of 10-week-old mice using a minimally invasive endotracheal instillation method. The mice were anesthetized by ketamine and xylazine (45 mg/kg and 8 mg/kg, respectively) and were suspended on a flat board and placed in a semi-recumbent position with the ventral surface and rostrum facing upwards. Using curved blade Kelly forceps, the tongue is gently and partially retracted rostrally and 50 μl of clodronate liposomes is placed in the back of the oral cavity, which is then aspirated by the animal. Control liposomes (50μl) alone were similarly administered in the control group. After 2 days of clodronate treatment, mice were reconstituted by i.t. instillation in a similar manner with differentiated bone marrow macrophages either from WT or TWIK2 KO at dose of 2×106 in a 50μl volume per mice. The mice were injected with i.p. LPS (20mg/Kg) after 24 h of macrophage reconstitution. The lungs were flushed and harvested after 24 h of LPS challenge. The efficiency of macrophage depletion was evaluated by sorting cells labeled with F4/80 and CD11b antibody via flow cytometry (see Figure S7).

QUANTIFICATION AND STATISTICAL ANALYSIS

Statistical comparisons were made using ordinary one-way ANOVA multiple comparisons with Prism 6 (GraphPad). Experimental values were reported as the means ± S.E.M (standard error of the mean). Significance between groups was labeled with asterisks indicating a statistically significant difference with the number of experiments indicated in parentheses.

Supplementary Material

Refer to Web version on PubMed Central for supplementary material.

Acknowledgments

References

Achan J, Talisuna AO, Erhart A, Yeka A, Tibenderana JK, Baliraine FN, Rosenthal PJ, D'Alessandro U. Quinine, an old anti-malarial drug in a modern world: role in the treatment of malaria. Malaria journal. 2011; 10:144. [PubMed: 21609473]

Bachmaier K, Toya S, Gao X, Triantafillou T, Garrean S, Park GY, Frey RS, Vogel S, Minshall R, Christman JW, et al. E3 ubiquitin ligase Cblb regulates the acute inflammatory response underlying lung injury. Nat Med. 2007; 13:920–926. [PubMed: 17618294]

Bobak N, Feliciangeli S, Chen CC, Ben Soussia I, Bittner S, Pagnotta S, Ruck T, Biel M, Wahl-Schott C, Grimm C, et al. Recombinant tandem of pore-domains in a Weakly Inward rectifying K+ channel 2 (TWIK2) forms active lysosomal channels. Scientific reports. 2017; 7:649. [PubMed: 28381826]

Broz P, Dixit VM. Inflammasomes: mechanism of assembly, regulation and signalling. Nat Rev Immunol. 2016; 16:407–420. [PubMed: 27291964]

Buell G, Lewis C, Collo G, North RA, Surprenant A. An antagonist-insensitive P2x receptor expressed in epithelia and brain. EMBO J. 1996; 15:55–62. [PubMed: 8598206]

Burns K, Martinon F, Tschopp J. New insights into the mechanism of IL-1beta maturation. Curr Opin Immunol. 2003; 15:26–30. [PubMed: 12495729]

Chan FK, Moriwaki K, De Rosa MJ. Detection of necrosis by release of lactate dehydrogenase activity. Methods Mol Biol. 2013; 979:65–70. [PubMed: 23397389]

Chavez RA, Gray AT, Zhao BB, Kindler CH, Mazurek MJ, Mehta Y, Forsayeth JR, Yost CS. TWIK-2, a new weak inward rectifying member of the tandem pore domain potassium channel family. J Biol Chem. 1999; 274:7887–7892. [PubMed: 10075682]

Chen GY, Nunez G. Sterile inflammation: sensing and reacting to damage. Nat Rev Immunol. 2010; 10:826–837. [PubMed: 21088683]

Chessell IP, Simon J, Hibell AD, Michel AD, Barnard EA, Humphrey PP. Cloning and functional characterisation of the mouse P2x7 receptor. FEBS Lett. 1998; 439:26–30. [PubMed: 9849870]

Cuenca AG, Delano MJ, Kelly-Scumpia KM, Moldawer LL, Efron PA. Cecal ligation and puncture. Curr Protoc Immunol. 2010 Chapter 19, Unit 19 13.

David J, , Aidley PRS. Ion Channels Great Britain: Cambridge University Press; 1996

de Torre-Minguela C, Barbera-Cremades M, Gomez AI, Martin-Sanchez F, Pelegrin P. Macrophage activation and polarization modify P2x7 receptor secretome influencing the inflammatory process. Scientific reports. 2016; 6:22586. [PubMed: 26935289]

Di A, Krupa B, Nelson DJ. Calcium-G protein interactions in the regulation of macrophage secretion. J Biol Chem. 2001; 276:37124–37132. [PubMed: 11479305]

dos Santos G, Kutuzov MA, Ridge KM. The inflammasome in lung diseases. Am J Physiol Lung Cell Mol Physiol. 2012; 303:L627–633. [PubMed: 22904168]

Enyedi P, Czirjak G. Molecular background of leak K+ currents: two-pore domain potassium channels. Physiol Rev. 2010; 90:559–605. [PubMed: 20393194]

Franchi L, Kanneganti TD, Dubyak GR, Nunez G. Differential requirement of P2x7 receptor and intracellular K+ for caspase-1 activation induced by intracellular and extracellular bacteria. J Biol Chem. 2007; 282:18810–18818. [PubMed: 17491021]

Franchi L, Munoz-Planillo R, Nunez G. Sensing and reacting to microbes through the inflammasomes. Nat Immunol. 2012; 13:325–332. [PubMed: 22430785]

Grailer JJ, Canning BA, Kalbitz M, Haggadone MD, Dhond RM, Andjelkovic AV, Zetoune FS, Ward PA. Critical role for the NLRP3 inflammasome during acute lung injury. J Immunol. 2014; 192:5974–5983. [PubMed: 24795455]

Gross CJ, Mishra R, Schneider KS, Medard G, Wettmarshausen J, Dittlein DC, Shi H, Gorka O, Koenig PA, Fromm S, et al. K(+) Efflux-Independent NLRP3 Inflammasome Activation by Small Molecules Targeting Mitochondria. Immunity. 2016; 45:761–773. [PubMed: 27692612]

Howrylak JA, Nakahira K. Inflammasomes: Key Mediators of Lung Immunity. Annu Rev Physiol. 2017; 79:471–494. [PubMed: 28192059]

Hume RI, Thomas SA. Multiple actions of adenosine 5'-triphosphate on chick skeletal muscle. J Physiol. 1988; 406:503–524. [PubMed: 2474071]

Kahlenberg JM, Dubyak GR. Mechanisms of caspase-1 activation by P2x7 receptor-mediated K+ release. Am J Physiol Cell Physiol. 2004; 286:C1100–1108. [PubMed: 15075209]

Katsnelson MA, Rucker LG, Russo HM, Dubyak GR. K+ Efflux Agonists Induce NLRP3 Inflammasome Activation Independently of Ca2+ Signaling. J Immunol. 2015; 194:3937–3952. [PubMed: 25762778]

Latz E, Xiao TS, Stutz A. Activation and regulation of the inflammasomes. Nat Rev Immunol. 2013; 13:397–411. [PubMed: 23702978]

Leed A, DuBay K, Ursos LM, Sears D, De Dios AC, Roepe PD. Solution structures of antimalarial drug-heme complexes. Biochemistry. 2002; 41:10245–10255. [PubMed: 12162739]

Lloyd EE, Crossland RF, Phillips SC, Marrelli SP, Reddy AK, Taffet GE, Hartley CJ, Bryan RM Jr. Disruption of K(2P)6.1 produces vascular dysfunction and hypertension in mice. Hypertension. 2011; 58:672–678. [PubMed: 21876070]

Lloyd EE, Marrelli SP, Namiranian K, Bryan RM Jr. Characterization of TWIK-2, a two-pore domain K+ channel, cloned from the rat middle cerebral artery. Experimental biology and medicine. 2009; 234:1493–1502. [PubMed: 19934370]

Lu A, Magupalli VG, Ruan J, Yin Q, Atianand MK, Vos MR, Schroder GF, Fitzgerald KA, Wu H, Egelman EH. Unified polymerization mechanism for the assembly of ASC-dependent inflammasomes. Cell. 2014; 156:1193–1206. [PubMed: 24630722]

Munoz-Planillo R, Kuffa P, Martinez-Colon G, Smith BL, Rajendiran TM, Nunez G. K(+) efflux is the common trigger of NLRP3 inflammasome activation by bacterial toxins and particulate matter. Immunity. 2013; 38:1142–1153. [PubMed: 23809161]

Pandit LM, Lloyd EE, Reynolds JO, Lawrence WS, Reynolds C, Wehrens XH, Bryan RM. TWIK-2 channel deficiency leads to pulmonary hypertension through a rho-kinase-mediated process. Hypertension. 2014; 64:1260–1265. [PubMed: 25245387]

Patel AJ, Maingret F, Magnone V, Fosset M, Lazdunski M, Honore E. TWIK-2, an inactivating 2P domain K+ channel. J Biol Chem. 2000; 275:28722–28730. [PubMed: 10887187]

Pelegrin P, Surprenant A. Pannexin-1 mediates large pore formation and interleukin-1beta release by the ATP-gated P2x7 receptor. EMBO J. 2006; 25:5071–5082. [PubMed: 17036048]

Pelegrin P, Surprenant A. The P2x(7) receptor-pannexin connection to dye uptake and IL-1beta release. Purinergic signalling. 2009; 5:129–137. [PubMed: 19212823]

Petrilli V, Papin S, Dostert C, Mayor A, Martinon F, Tschopp J. Activation of the NALP3 inflammasome is triggered by low intracellular potassium concentration. Cell Death Differ. 2007; 14:1583–1589. [PubMed: 17599094]

Rassendren F, Buell GN, Virginio C, Collo G, North RA, Surprenant A. The permeabilizing ATP receptor, P2x7. Cloning and expression of a human cDNA. J Biol Chem. 1997; 272:5482–5486. [PubMed: 9038151]

Schroder K, Tschopp J. The inflammasomes. Cell. 2010; 140:821–832. [PubMed: 20303873]

Sheldon R, Duff H, Koshman ML. Antiarrhythmic activity of quinine in humans. Circulation. 1995; 92:2944–2950. [PubMed: 7586264]

Shieh CC, Coghlan M, Sullivan JP, Gopalakrishnan M. Potassium channels: molecular defects, diseases, and therapeutic opportunities. Pharmacol Rev. 2000; 52:557–594. [PubMed: 11121510]

Solle M, Labasi J, Perregaux DG, Stam E, Petrushova N, Koller BH, Griffiths RJ, Gabel CA. Altered cytokine production in mice lacking P2x(7) receptors. J Biol Chem. 2001; 276:125–132. [PubMed: 11016935]

Srinivasula SM, Poyet JL, Razmara M, Datta P, Zhang Z, Alnemri ES. The PYRIN-CARD protein ASC is an activating adaptor for caspase-1. J Biol Chem. 2002; 277:21119–21122. [PubMed: 11967258]

Surprenant A, Rassendren F, Kawashima E, North RA, Buell G. The cytolytic P2Z receptor for extracellular ATP identified as a P2x receptor (P2x7). Science. 1996; 272:735–738. [PubMed: 8614837]

Thomas SA, Hume RI. Permeation of both cations and anions through a single class of ATP-activated ion channels in developing chick skeletal muscle. J Gen Physiol. 1990; 95:569–590. [PubMed: 1692581]

Valera S, Hussy N, Evans RJ, Adami N, North RA, Surprenant A, Buell G. A new class of ligand-gated ion channel defined by P2x receptor for extracellular ATP. Nature. 1994; 371:516–519. [PubMed: 7523951]

Wang W, Zhang X, Gao Q, Lawas M, Yu L, Cheng X, Gu M, Sahoo N, Li X, Li P, et al. A voltage-dependent K(+) channel in the lysosome is required for refilling lysosomal Ca(2+) stores. J Cell Biol. 2017; 216:1715–1730. [PubMed: 28468834]

Wegiel B, Larsen R, Gallo D, Chin BY, Harris C, Mannam P, Kaczmarek E, Lee PJ, Zuckerbraun BS, Flavell R, et al. Macrophages sense and kill bacteria through carbon monoxide-dependent inflammasome activation. J Clin Invest. 2014; 124:4926–4940. [PubMed: 25295542]

Weisser SB, van Rooijen N, Sly LM. Depletion and reconstitution of macrophages in mice. Journal of visualized experiments : JoVE. 2012:4105. [PubMed: 22871793]

Wu J, Yan Z, Schwartz DE, Yu J, Malik AB, Hu G. Activation of NLRP3 inflammasome in alveolar macrophages contributes to mechanical stretch-induced lung inflammation and injury. J Immunol. 2013; 190:3590–3599. [PubMed: 23436933]

Zhang X, Goncalves R, Mosser DM. The isolation and characterization of murine macrophages. Curr Protoc Immunol. 2008 Chapter 14, Unit 14 11.

Highlights

- Macrophage NLRP3 inflammasome activation is inhibited by potassium channel inhibition

- TWIK2 is a potassium efflux channel required for NLRP3 inflammasome activation

- Genetic deletion of TWIK2 prevents endotoxemia-induced inflammatory lung injury

- P2X7 receptor and TWIK2 act in cooperation to regulate NLRP3 inflammasome activation
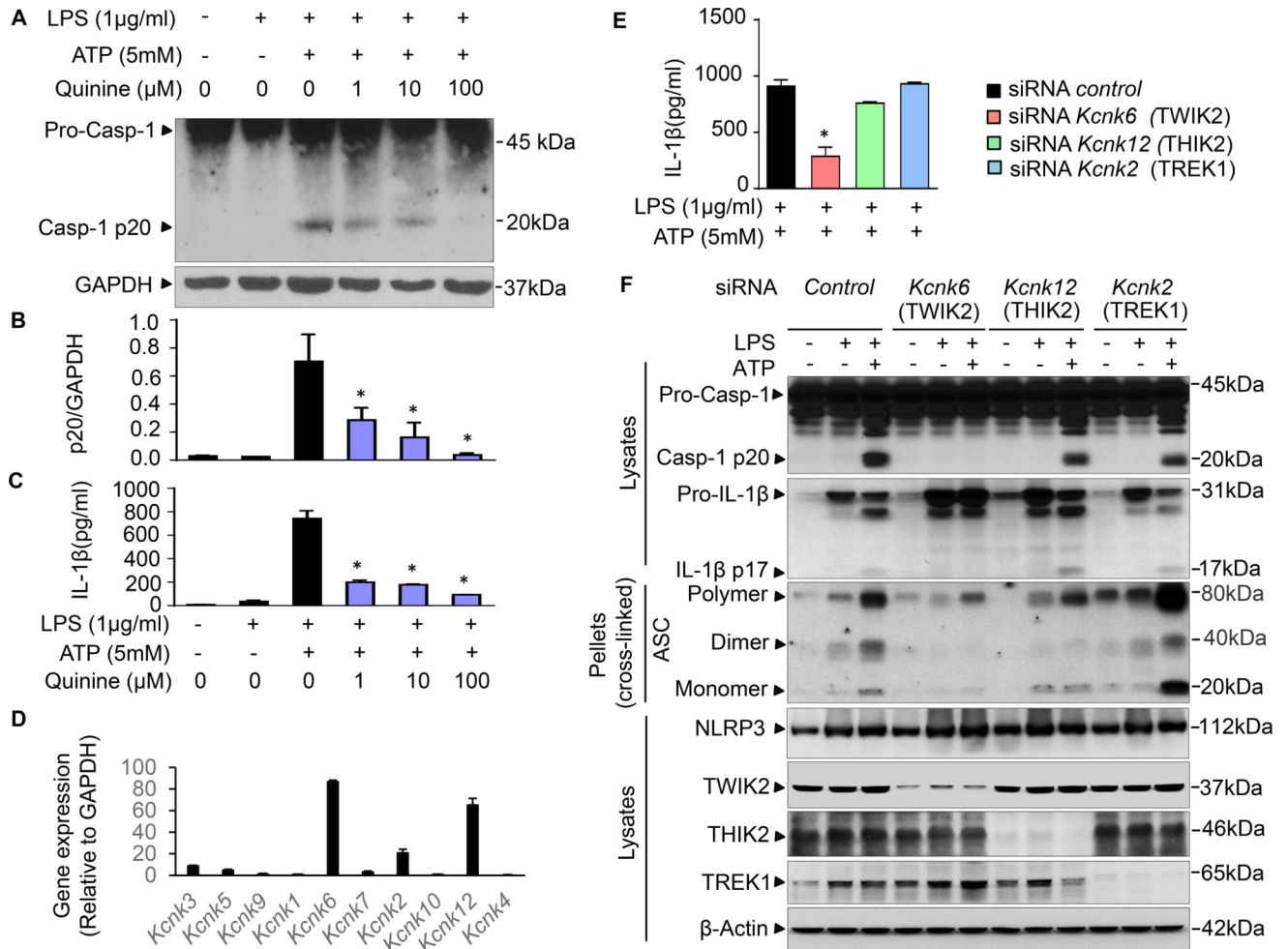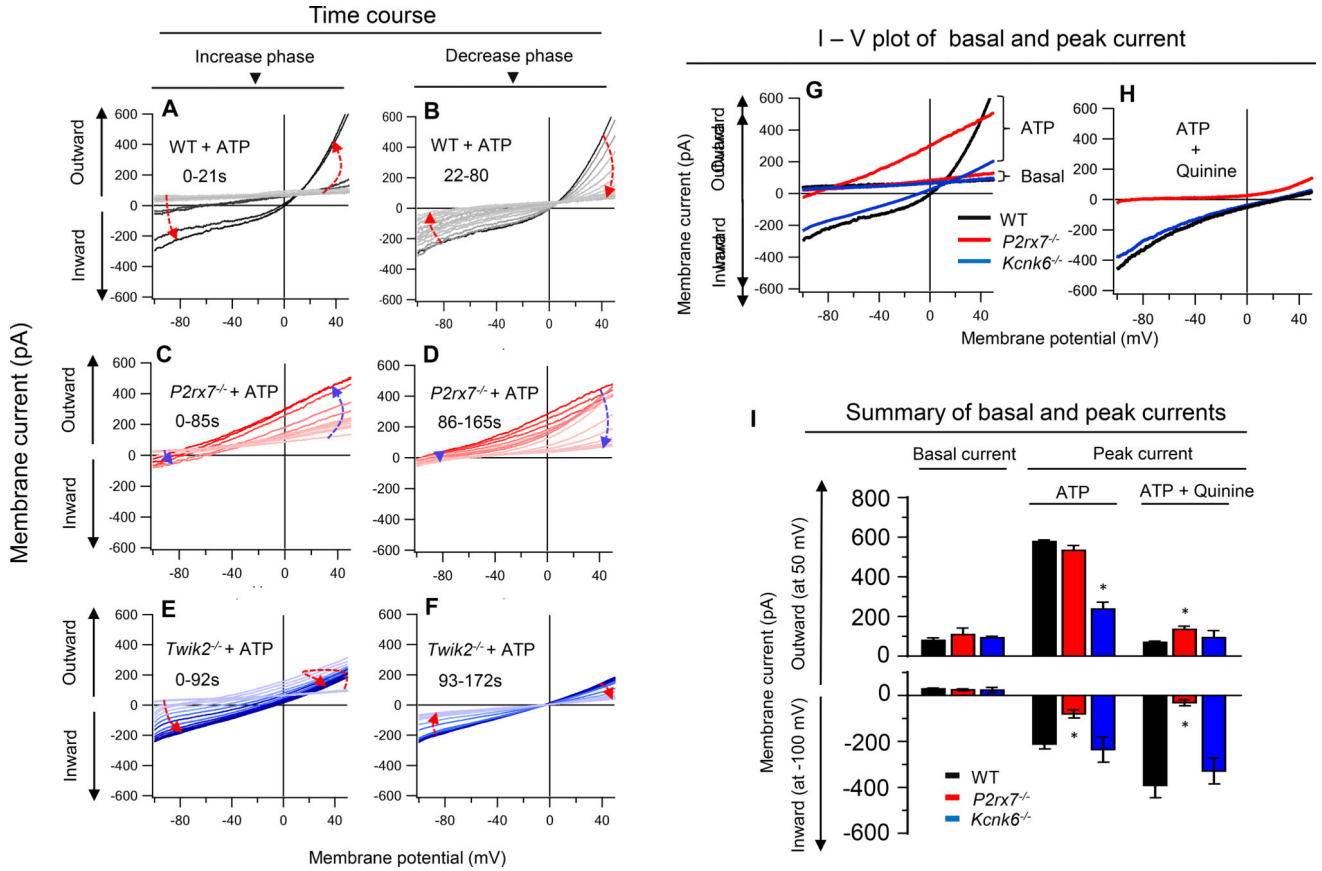
Figure 1. TWIK2 mediated quinine sensitive NLRP3 inflammasome activation in macrophages

A – **C**: Quinine inhibits ATP-induced NLRP3 inflammasome activation. Mouse bone marrow derived macrophages (BMDMs) were primed with LPS for 3h and subsequently challenged with ATP for 30min. Cell lysates were immunoblotted with caspase-1 p20 antibody (**A**) and results are summarized in **B** (* $p < 0.05$ compared with group treated with LPS and ATP but without quinine, n = 3). IL-1β release in supernatants was measured using ELISA method (**C**, * $p < 0.05$ compared with group treated with LPS and ATP but without quinine, n = 3). **D**: mRNA of various two-pore domain K channel (K2P) in BMDMs were assessed by qRT-PCR for the following: *Kcnk1* (encoding TWIK1), *Kcnk6* (encoding TWIK2), *Kcnk7* (encoding TWIK3); TWIK1, TWIK2, TWIK3: 2 pore domain weak inwardly rectifying K^+ channel 1, 2, and 3; *Kcnk3* (encoding TASK1), *Kcnk5* (encoding TASK2), *Kcnk9* (encoding TASK3); TASK1, TASK2, TASK3: TWIK related acid-sensitive K^+ channel 1, 2, and 3; *Kcnk2* (encodingTREK1), *Kcnk10* (encodingTREK2); TREK1, TREK2: TWIK related K^+ channel 1 and 2; *Kcnk12* (encodingTHIK2: 2 pore domain halothane-inhibited K^+ channel 2); *Kcnk4* (encoding TRAAK: TWIK related arachidonic acid-stimulated K^+ channel). *Kcnk6*, *Kcnk2* and *Kcnk12* exhibited the highest expression (n = 3). **E** – **F**: TWIK2 silenced by siRNA inhibited ATP-induced NLRP3 inflammasome activation. Mouse J774A.1 (cell line) MΦs were treated with control siRNA or siRNA

targeting *Kcnk6*, *Kcnk2* and *Kcnk12*, respectively. IL-1β release in supernatants was monitored with ELISA method (**E**, * $p < 0.05$ compared with siRNA control group, n = 3) and cell lysates or pellets were immunoblotted with indicated antibodies (**F**, representative of 3 independent experiments). NLRP3: nucleotide-binding oligomerization domain-like receptor (NLR) containing pyrin domain 3; ASC: apoptosis-associated speck-like protein containing a carboxy-terminal caspase recruitment domain (CARD). Please also see Figure S1, S2, S3 and S4.
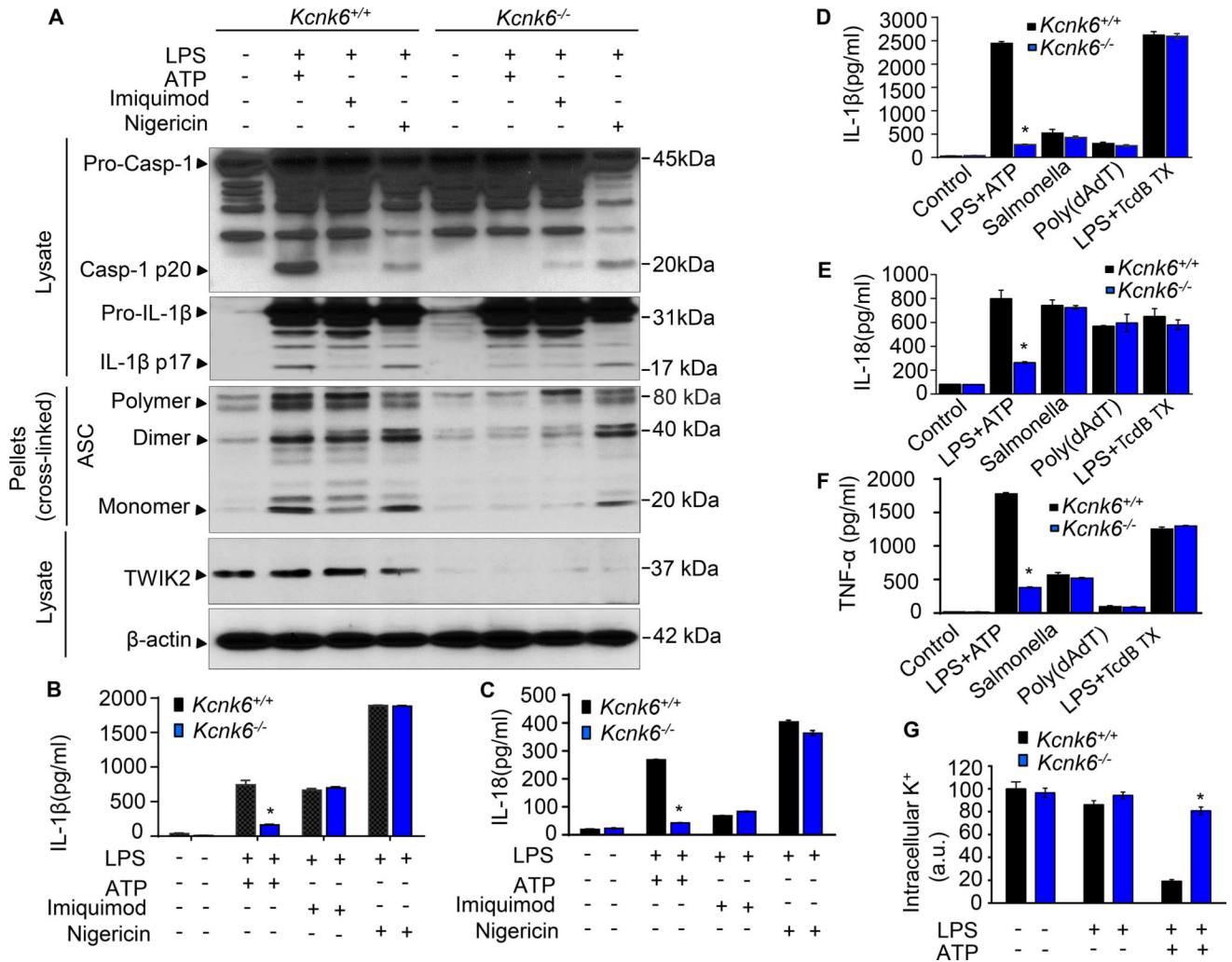
Figure 2. TWIK2 mediated and P2X7 independent K^+ efflux in macrophages

A – **F**: Representative current traces at ramp voltages of whole cell patch clamp recordings with time in BMDMs from wild type (WT, **A** and **B**, 7 independent experiments), $P2rx7^{-/-}$ (**C** and **D**, 5 independent experiments) and $Kcnk6^{-/-}$ (**E** and **F**, 6 independent experiments) mice. Cells were bathed in solutions with K^+ as the major outward current and Na^+ and Ca^{2+} as the major inward current. Whole cell current was elicited with ramp voltages running from −110 mV to +50 mV within 200 ms were applied to cells with an interval of 1s. The direction of currents was indicated by straight black arrows. The "increased phase" means the currents increase with time from basal level to the peak of positive (outward) current or to the peak of negative (inward) current (indicated by color arrows). The "decreased phase" means the currents decrease with time from the peak of the outward currents or from the peak of inward) current to the basal level (indicated by color arrows); **G** – **H**: Comparison of basal and ATP-induced peak current in the absence of quinine (**G** as described in **A**) and of ATP-induced peak current in the presence of quinine (**H**, representative of 3 independent experiments) in the different cells as indicated. The amplitudes of the outward peak currents (under 50 mV) and inward peak current (under −100 mV) from experiments described in **A** – **F** and **H** are summarized in **I** (* $p < 0.05$ compared with WT group in each condition). Please also see Figure S2, S3, S4 and Figure S5.

Figure 3. TWIK2 mediated K$^+$ efflux is required for NLRP3 inflammasome activation

A – **C**. TWIK2 deletion (*Kcnk6$^{-/-}$*) prevented ATP induced NLRP3 inflammasome activation in BMDMs but had no effect on neither imiquimod nor nigericin activated responses. Cells were primed with LPS (3h) and subsequently challenged with ATP (5 mM) or Imiquimod (10 μg/ml) or Nigericin (10 μg/ml) for 30 min. Cell lysates or pellets were immunoblotted with indicated antibodies (**A**, representative results of 3 independent experiments). IL-1β and IL-18 release in supernatants was measured using ELISA method (**B** and **C**, * p < 0.05 compared with *Kcnk6$^{+/+}$* plus LPS and ATP group, n = 3). **D** – **F**. *Kcnk6* deletion prevented NLLRP3 (not NLRC4, AIM2, or pyrin) inflammasome activation in BMDMs. BMDMs from *Kcnk6$^{+/+}$* and *Kcnk6$^{-/-}$* mice were either used in an unprimed state or primed with LPS and then challenged with ATP (5mM) for 30 min or Salmonella (5 moi, to activate NLRC4) for 2h or poly (dAdT), to activate AIM2) (2 μg/ml) for 2h or TcdB toxin (0.5 μg/ml, to activate pyrin) for 3h. IL-1β (**D**), IL-18 (**E**) and TNF-α (**F**) concentrations in cell-free supernatants were quantified by ELISA. NLRC4: NLR family, CARD domain containing 4; AIM2: absent in melanoma 2. * p < 0.05 compared with *Kcnk6$^{+/+}$* plus LPS and ATP group, n = 3. **G**. TWIK2 deletion prevented ATP-induced decrease in intracellular potassium (K$^+$) concentration. BMDMs were primed with LPS (3h)

and then treated with ATP (30min). Intracellular K^+ was examined by FluxOR™ II green potassium ion channel assay. * $p < 0.05$ compared with *Kcnk6*$^{+/+}$ plus LPS and ATP group, n = 6. Please also see Figure S5 D – E and Figure S6 A – B.
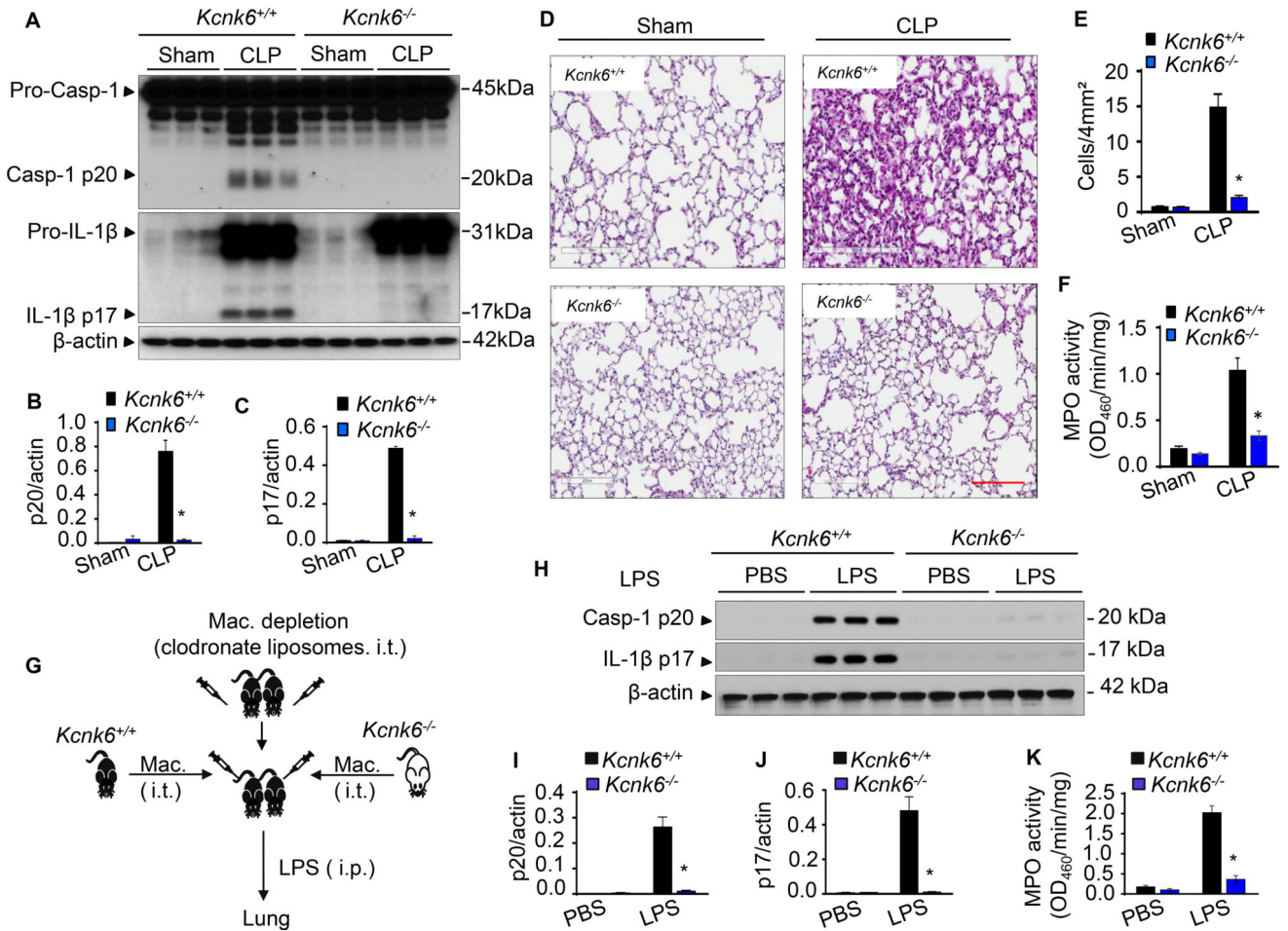
Figure 4. TWIK2 deficiency prevents sepsis-induced NLRP3 inflammasome activation and inflammatory lung injury in mice

A – **F**: Deletion of *Kcnk6* (encoding TWIK2) prevents sepsis-induced NLRP3 inflammasome activation and inflammatory lung injury in mice. Murine lung inflammatory injury resulting from polymicrobial sepsis was induced through cecal ligation puncture (CLP) in both *Kcnk6*^{+/+} and *Kcnk6*^{−/−} mice. NLRP3 inflammasome activation (indicated by caspase 1 activation and IL-1β maturation) in the murine lung was assessed by Immunoblotting (**A**) and quantified in **B** and **C** (* $p < 0.05$ compared with *Kcnk6*^{+/+} CLP group, n = 3). Representative H&E images of lung sections from 3 independent experiments are shown in **D**. Scale bars: 200 μm. Lung injury shown in **D** was evaluated by quantification of inflammatory cells in alveoli (per 4mm^2 using the *Fiji* image analysis software) in **E**, and MPO measurements of lung tissue are shown in **F** (* $p < 0.05$ compared with *Kcnk6*^{+/+} CLP group, n = 3). **G** – **K**: *Kcnk6* deletion in macrophages prevents sepsis-induced NLRP3 inflammasome activation and inflammatory lung injury in mice. Lung macrophages (Mac) were depleted with clodronate liposomes and then reconstituted intratracheally with BMDMs either from *Kcnk6*^{+/+} or *Kcnk6*^{−/−} mice as illustrated in **G**. The mice were injected with LPS (intra-peritoneal injection, i.p.) after 24 h of macrophage reconstitution. Lungs were harvested for evaluation of NLRP3 inflammasome activation (**H** – **J**) and neutrophil

infiltration by checking MPO concentration (**K**), * p < 0.05 compared with *Kcnk6*$^{+/+}$ LPS group, n = 3. Please also see Figure S6C.
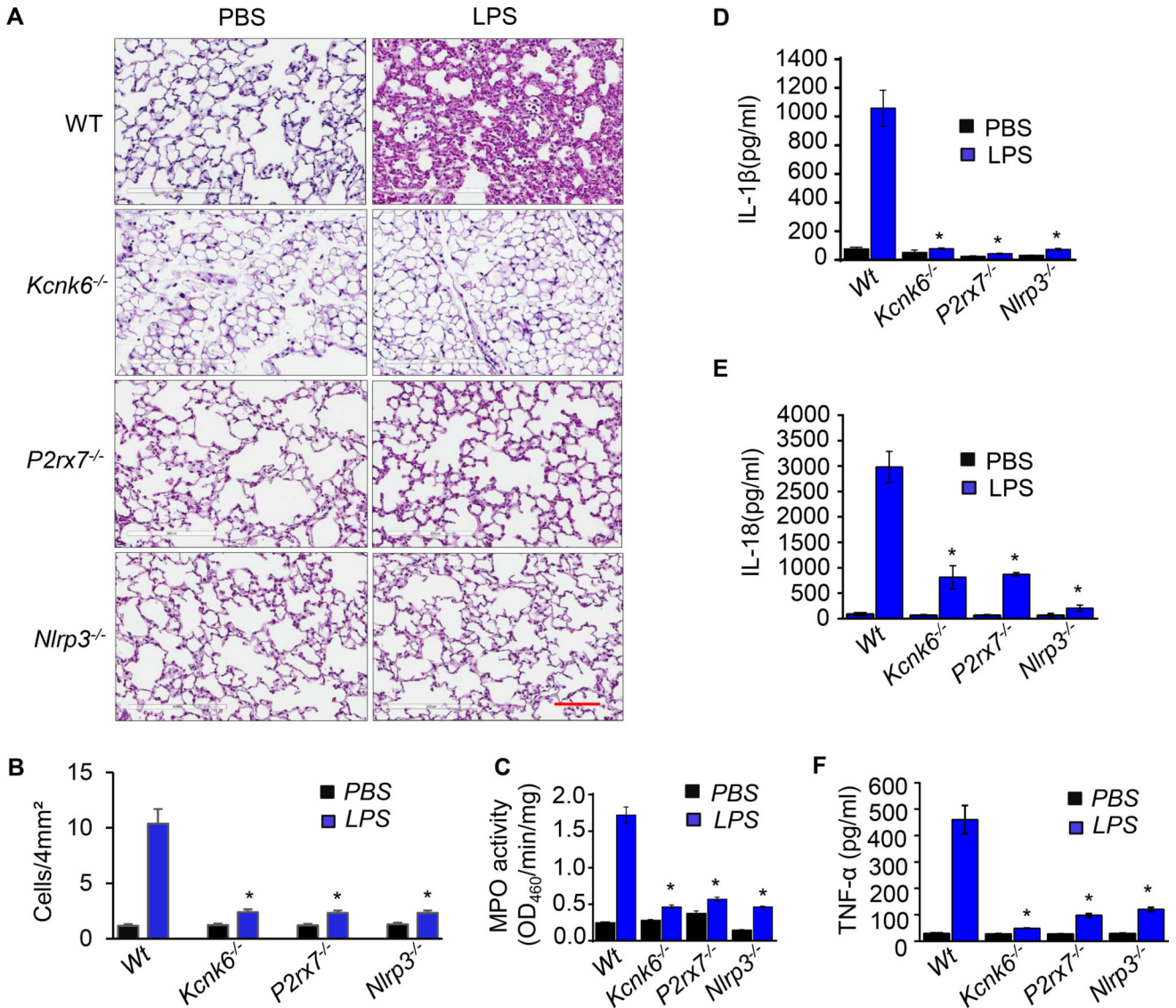
Figure 5. Prevention of LPS-induced inflammation by TWIK2 deletion is mimicked by deleting P2X7 or NLRP3 in mice

A – C: Prevention of LPS-induced lung inflammation by TWIK2 deficiency renders similar responses to LPS in P2X7 or NLRP3 deletion mice. Mouse lung inflammation was induced by intra-peritoneal injection (i.p.) of LPS and histological sections of lungs from wild type (WT), TWIK2 deficiency (*Kcnk6*$^{-/-}$), P2X7 deficiency (*P2rx7*$^{-/-}$) and NLRP3 deficiency (*Nlrp3*$^{-/-}$) were stained with hematoxylin and eosin (HE) 24h of LPS injection to assess immune cell infiltration (**A**, representative results of 3 independent experiments; scale bars = 100 μm). Lung injury was evaluated by inflammatory cell quantification in alveoli per 4mm^2 using the *Fiji* image analysis software (**B**) and lung myeloperoxidase (MPO) activity (**C**). * p < 0.05 compared with WT LPS group, n = 3. **D – F**: TWIK2 deficiency prevented LPS-induced cytokine increases in serum which was phenocopied in *P2rx7*$^{-/-}$ or *Nlrp3*$^{-/-}$ mice. Concentrations of IL-1β, IL –18, and TNF-α in the mice mentioned in **A – C** were evaluated with ELISA methods. * p < 0.05 compared with WT LPS group, n = 3.
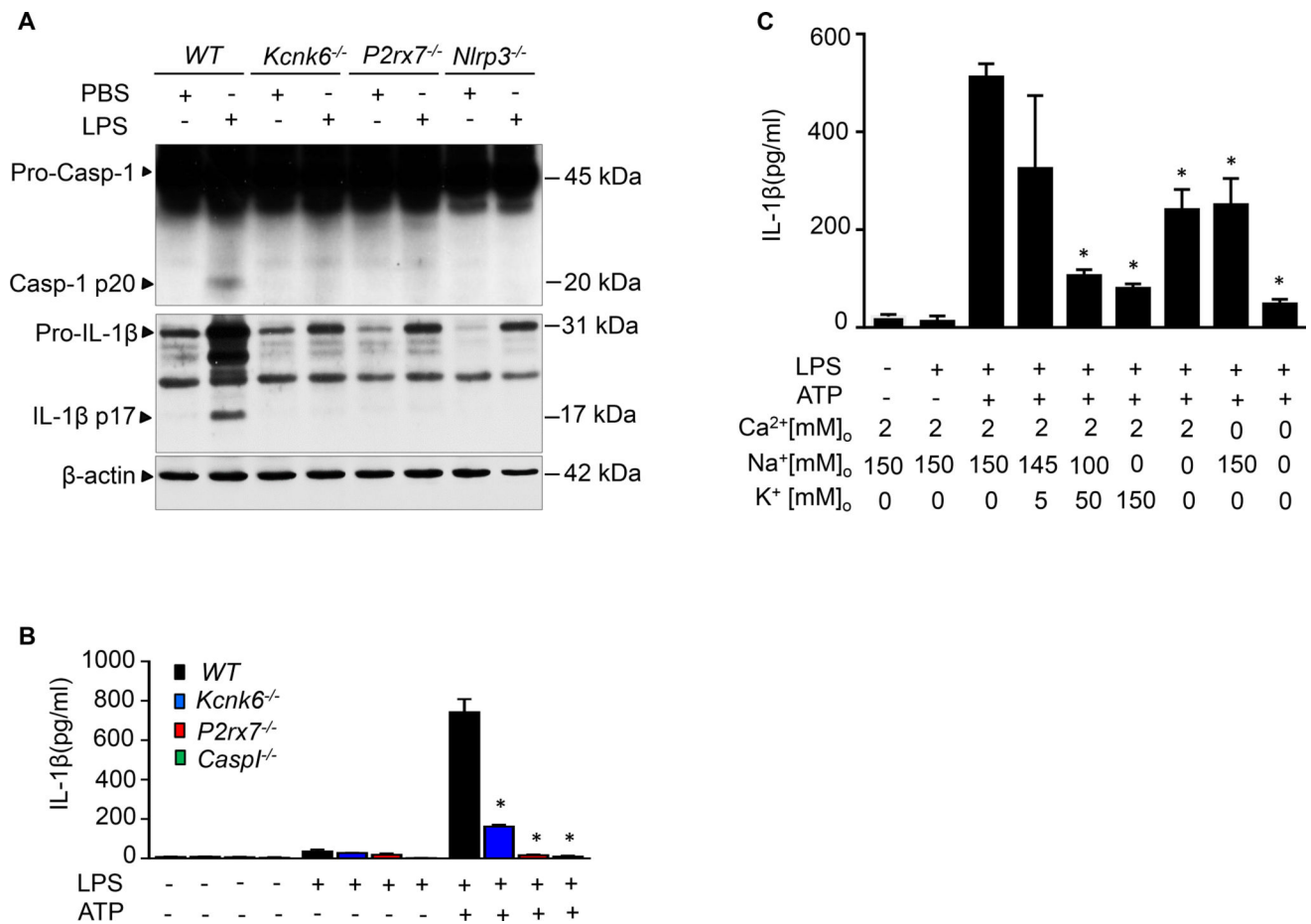
Figure 6. P2X7 mediated influx of cations functions in cooperation with K⁺ efflux through TWIK2 to induce NLRP3 inflammasome activation in macrophages

A: TWIK2 deficiency prevents LPS-induced NLRP3 inflammasome activation similar to what is observed with P2X7 or NLRP3 deficiency in mice. Mouse lung inflammasome activation was induced by intra-peritoneal injection (i.p.) of LPS for 1 day. NLRP3 inflammasome activation (as indicated by caspase-1 activation and IL-1β maturation) was assessed in murine lungs using immunoblotting. Representative results from 3 independent experiments are shown. **B**: TWIK2 deficiency (*Kcnk6⁻/⁻*) prevented LPS-primed and ATP-induced NLRP3 inflammasome activation, and this response was similar what was seen in P2X7 deficient (*P2rx7⁻/⁻*) and caspase 1 deficient (*Casp1⁻/⁻*) cells (BMDMs). * p < 0.05 compared with WT plus LPS and ATP group, n = 3. **C**: Depletion of extracellular calcium (Ca²⁺) alone or sodium (Na⁺) alone only partly inhibited ATP-induced NLRP3 inflammasome activation. BMDMs were primed with LPS and then stimulated with ATP at different extracellular concentration of K⁺, Ca²⁺ and Na⁺ as indicated. * p < 0.05 compared with LPS plus ATP but without extracellular K⁺ ([K⁺]$_O$ = 0), n = 3 – 12. IL-1β release in BMDMs was evaluated by ELISA method.